

Fabrication and Mechanical Properties of SiC Platelet Reinforced Mullite Matrix Composites

H. R. Rezaie, W. M. Rainforth and W. E. Lee*

Department of Engineering Materials, The University of Sheffield, Mappin Street, Sheffield S1 3JD, UK

(Received 1 July 1998; accepted 14 November 1998)

Abstract

Hot-pressing of mullite and SiC–mullite matrix composites was performed at temperatures and pressures between 1500 and 1650°C and 5 and 15 MPa, respectively. Composites were produced using different precursors; sol–gel derived mullite and kaolinite/ α -alumina. The precursor did not strongly affect the optimum density achieved, reaching 97.5% of theoretical for a 20 vol% SiC addition in both cases. The SiC platelet addition impaired densification kinetics in all composites compared to mullite monoliths. Fracture toughness, measured by the indentation strength in bending technique, was marginally higher for the sol–gel precursor material in both monolith and composite. Fracture toughness increased with SiC content for both materials. For example, for the sol-gel precursor material it increased from 2.9 ± 0.1 MPa $m^{1/2}$ for the monolith to 3.9 ± 0.1 MPa $m^{1/2}$ for the 20 vol% SiC composite. Similarly, hardness increased with SiC addition for both materials, but the hardness of the sol–gel material was greater than that of the kaolinite + α -alumina material for all compositions. The relationship between microstructure and mechanical properties is discussed.

© 1999 Published by Elsevier Science Limited. All rights reserved

Keywords: composites, mullite, SiC, platelets, toughness, hot pressing.

1 Introduction

Monolithic mullite bodies suffer from low values of both bend strength (150–500 MPa) and fracture toughness (1.5–3.0 MPa $m^{1/2}$) at room temperature.¹ Reinforcement with high-strength second phases such as SiC whiskers by hot pressing, has shown promising improvements.² Silicon carbide

whiskers have been incorporated into numerous ceramic matrices in an attempt to improve their mechanical properties, in particular their resistance to catastrophic failure. However, two potential drawbacks to the use of whiskers have been identified. Firstly, their presence has a detrimental effect on the densification processes and secondly, they have been shown to be a potential health hazard if they have $< 1 \mu\text{m}$ diameter, as they can then be ingested into the lungs.³ Platelets of equivalent size with one short and two long dimensions are thought to offer similar reinforcing capability but no health hazards since their shape precludes ingestion.

This study compares mullite monoliths and mullite–SiC platelet composites using mullite derived from kaolinite mixed with α -alumina, and from sol–gel processing of boehmite and colloidal silica precursors. The microstructural evolution of mullite is examined in the different systems as a function of processing temperature. In addition, the mechanical properties of SiC platelet reinforced mullite are examined and correlated to precursor process route and microstructure. Possible toughening mechanisms derived from the SiC addition are discussed.

2 Experimental Procedures

Figure 1 summarises the processing route used in this work. Homogeneous (well-mixed) powder is required for the production of dense mullite ceramics. In this study mullite powder was produced via two different methods, a sol–gel route, and use of kaolin with α -alumina precursors described in more detail elsewhere.⁴

Boehmite and colloidal silica were used to prepare the sol–gel powder.⁴ For the alternative route, English China Clay International Super Standard kaolinite clay was mixed with calcined Bayer process α -alumina to give stoichiometric mullite. Details of these routes are described in a previous paper.⁴ The

*To whom correspondence should be addressed.

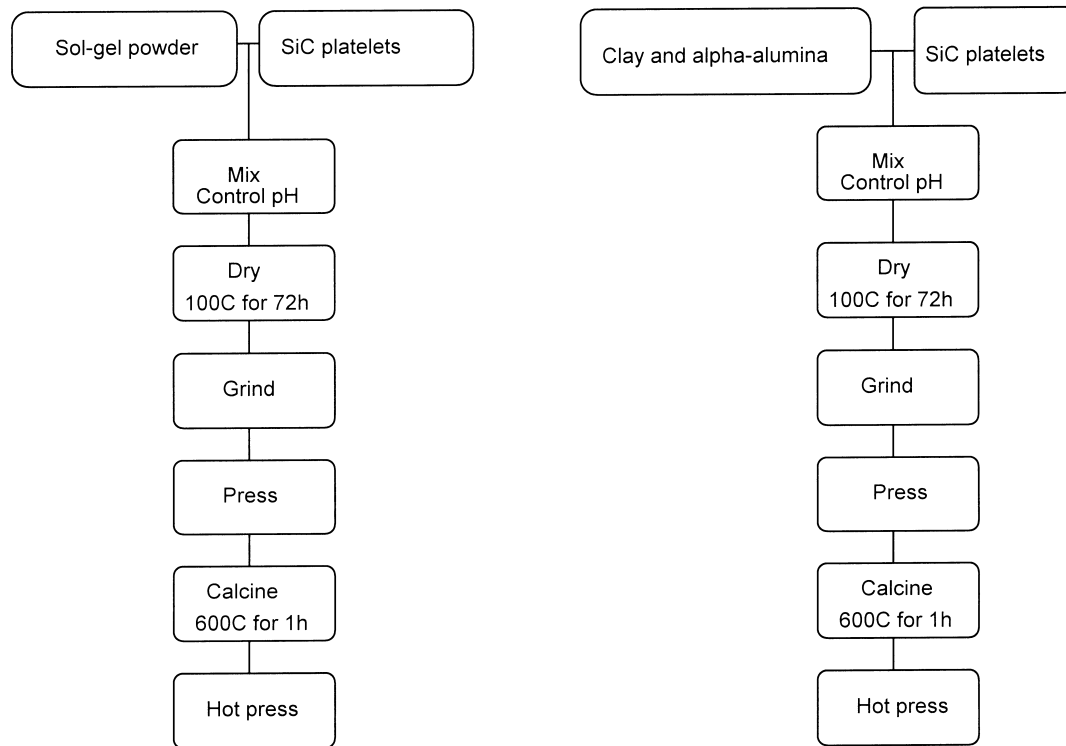


Fig. 1. Processing route to composites using sol-gel or clay/alumina precursors.

raw material compositions supplied by the manufacturers are given in Table 1.

α -SiC platelets with a wide variation in particle size were obtained from Newmet Ltd (Abbey Chambers, High Bridge Street, Waltham Abbey, Essex, EN9 1DF, UK) with nominal size -325 mesh ($5\text{--}70\ \mu\text{m}$ wide by $0.5\text{--}5\ \mu\text{m}$ thick). The mullite composition powders (from both sol-gel processing and kaolin with added α -alumina) were mixed with 10 and 20 vol% SiC platelets in pH stabilised suspensions by vigorous stirring for 24 h using a magnetic stirrer. All the starting materials were stabilized in distilled water with NH_4OH added to raise the pH to 10 to confer sufficient surface charge for electrostatic stabilization. The mixed suspension was stirred on a hot plate until a viscous consistency was obtained, followed by drying (at 100°C for 72 h) and milling (using an electrical agate mortar for 0.5 h).

Table 1. Chemical analyses of raw materials (supplied by the manufacturers)

Constituent	Boehmite (wt%)	Kaolin (wt%)	α - Al_2O_3 (wt%)
SiO_2	0.02	47	0.04
Al_2O_3	76.5	38	99.5
Fe_2O_3	0.01	0.39	0.02
TiO_2	—	0.03	—
CaO	—	0.10	0.03
MgO	—	0.22	—
K_2O	0.007	0.80	—
Na_2O	—	0.15	0.18
Loss on ignition	23	13.0	0.2

Mullite and SiC-mullite composite pellets were produced by uniaxially pressing the powders in a 30 mm diameter steel mould with 50 MPa pressure to give green compacts which were subsequently calcined at 600°C for 1 h.

Hot-pressing was carried out using an induction furnace (Inductoheat Banyard Ltd, Poole, Dorset, UK). The graphite dies used in the hot-press had a central cavity of 30 mm internal diameter with two graphite pistons of 30 mm external diameter to press the composite discs. The sample was completely sealed in the graphite die during hot-pressing and the die itself was surrounded by a powder mixture of graphite and zirconia to minimise oxidation of the die. Hot-pressing was carried out at a range of temperatures ($1500\text{--}1650^\circ\text{C}$) and pressures ($5\text{--}15\ \text{MPa}$), each for 1.5 h with a ramp of $20\ \text{K min}^{-1}$. All hot-pressed samples were allowed to naturally cool to room temperature in the furnace overnight (about $5\ \text{K min}^{-1}$).

The bulk density of the pellets was measured by Hg immersion and for each sintering temperature was measured twice on each of three samples, the results then being averaged. The general microstructure and grain size of the samples was determined by scanning electron microscopy (SEM) (Camscan Series 2), operating at 20 kV. Grain size was measured by the intercept method.⁵ The mean and one standard deviation were obtained from in excess of 500 grains for each sample condition.

For transmission electron microscopy (TEM), the samples were ground to 1 mm thickness and

then 3 mm dia. discs ultrasonically drilled from the slices were mechanically ground and polished to around 80–100 μm , and then dimpled to 20 μm centre thickness. These dimpled samples were then Ar ion milled at 6.0 kV until perforation, coated with carbon, and examined in a Philips EM 420 at 100 kV.

Vickers hardness was performed using the Vickers method (Vickers Armstrong Ltd, Crayford, Kent, UK, serial no. 254013) using a load of 10 kg. The sample was polished to an optical finish to enable crack types and lengths to be determined. The indentation time was ~ 15 s. A single datum was obtained from the average of 10 Vickers indents. Error bars represent one standard deviation.

Indentation fracture toughness is frequently used because of the simplicity of the approach and its good applicability.⁶ However, the technique has a number of drawbacks, namely, the small volume of material sampled, errors in measuring the crack length, the uncertainty of whether cracks are radial or Palmqvist, the presence of lateral cracking and the potential for time dependent crack propagation on removal of the indenter. Because of these factors, indentation strength in bending tests^{6,7} were undertaken. This allows a greater volume of material to be sampled and does not rely on the measurement of small cracks. Samples for this test were machined to 20 \times 10 \times 3 mm. The distance between the lower supporting points of the 3-point bend rig was 15 mm. The test surfaces were polished with increasingly finer abrasive paper down to 1200 mesh size. A Vickers indentation was made to provide a precrack, using a load of 10 kg at the centre of the prospective tensile face of each test piece, so that the diagonal of the indentation was aligned with respect to the longitudinal axis of the specimen. The crack morphology associated with the indent was checked prior to testing to ensure that no lateral cracking had occurred. The three-point-bend tests were performed using a Universal Mayes testing machine at room temperature under normal atmospheric conditions. The loading speed was 0.5 mm min⁻¹.

The fracture toughness, K_{IC} (MPa m^{1/2}), is determined from this technique using eqn (1),^{7,8} assuming a radial crack induced by the Vickers indent.

$$K_{\text{IC}} = \eta_{\text{V}}(E/H)^{1/8}(\sigma P^{1/3})^{3/4} \quad (1)$$

where $\eta_{\text{V}} = [256/27](\pi\Omega)^{3/2}\xi_{\text{V}}]^{1/4}$ is a geometrical constant E/H is the modulus-to-hardness ratio; σ is flexural strength (Pa); P is indentation load (N); Ω is a crack-geometry factor, and ξ_{V} is a constant for Vickers-produced radial cracks. The fracture surface

was examined in the SEM following the test and this confirmed that the pre-crack was radial in nature. At least four tests were performed for each material condition. The mean and one standard deviation are quoted.

3 Results

3.1 Densification

The bulk density of mullite and mullite with 10 and 20 vol% silicon carbide platelet additions from hot-pressed sol-gel (sg) powder is shown in Fig. 2. Density increased with increasing hot pressing temperature for mullite and mullite with 10 and 20 wt% SiC platelets from 1550 to 1650°C [Fig. 2(a)]. Maximum density (97.5% of theoretical density) was achieved after 1.5 h at 1650°C with 15 MPa pressure.

The bulk density of mullite and mullite with 10 and 20 vol% SiC platelet additions derived from kaolinite/ α -alumina by hot-pressing is shown in Fig. 3. The density increased significantly from 1500 to 1600°C, but levelled off above this temperature. As in Fig. 2(a) a decrease in density was found as platelet addition increased. A maximum density of 97.5% of theoretical was achieved after 1.5 h at 15 MPa pressure at 1600°C. The effect of applied pressure at 1600°C is shown [Fig. 3(b)]. Along with Fig. 2(b) these data show that the effect of applied pressure on final density after 1.5 h is not significant for mullite monoliths, and the mullite has almost reached full density after 1.5 h even with the lower pressures. However, applied pressure had a more significant effect on improving density in mullite with SiC platelet additions.

Maximum density for mullite and mullite with 10 and 20 vol% SiC platelets derived from kaolinite/ α -alumina occurred at a lower temperature [1600°C, Fig. 3(a)] than mullite and mullite with 10 and 20 vol% SiC platelets derived from sol-gel processing [1650°C, Fig. 2(a)].

3.2 Microstructural characterisation

The microstructure of hot pressed mullite pellets from sol-gel derived powder shows equiaxed mullite grains of a size about $1.7 \pm 0.3 \mu\text{m}$ after 1.5 h at 1650°C with 15 MPa pressure (Fig. 4). TEM revealed a glassy phase at some triple junctions, which occasionally extended along the grain boundaries. EDS (in the TEM) was used to examine the composition of mullite grains and the glassy phase in sol-gel pellets after 1.5 h at 1650°C with 15 MPa pressure. EDS confirmed the grains to be 3:2 mullite and indicated that the glass was predominantly silica.

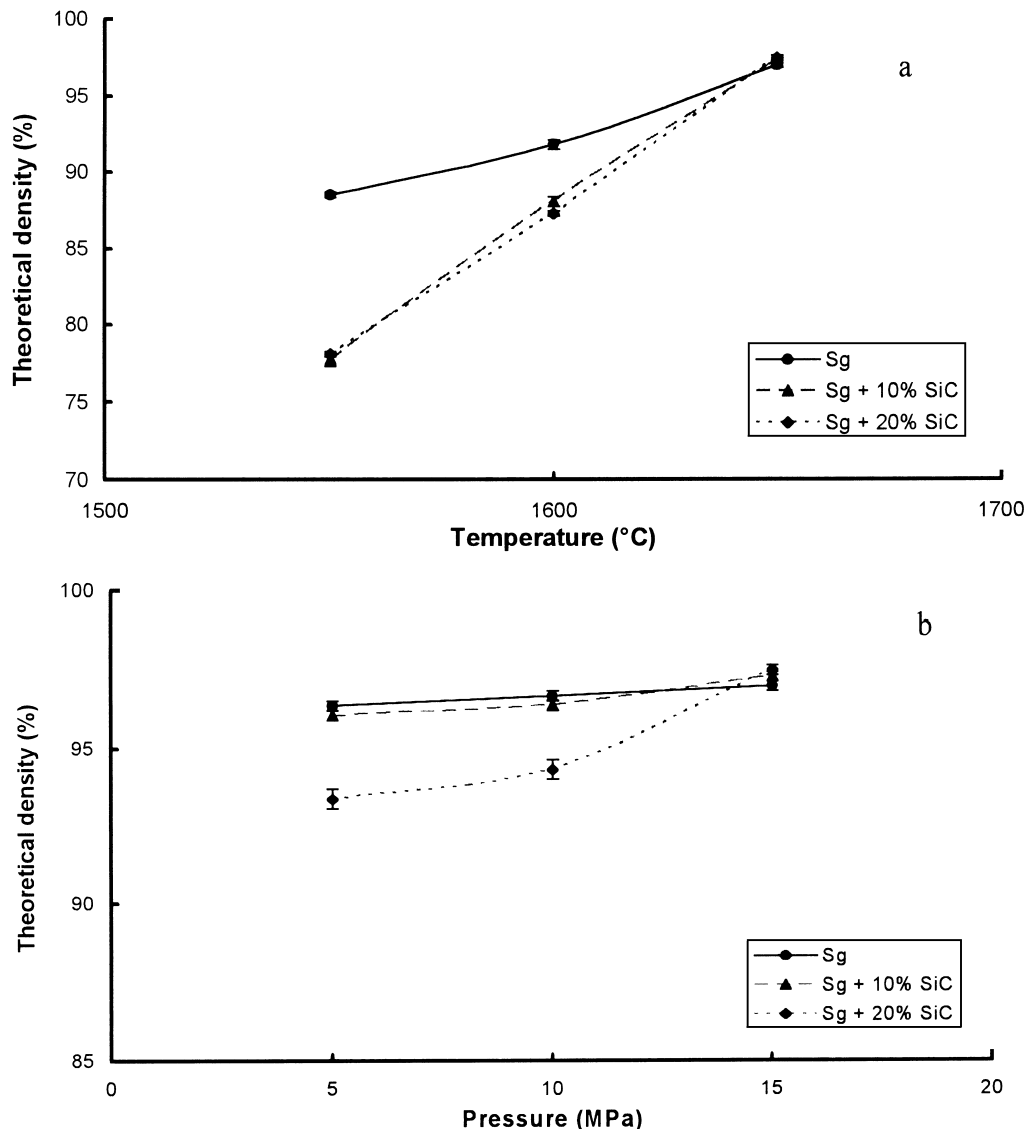


Fig. 2. Bulk density of mullite (sg) pellets derived from sol-gel powder hot pressed 1.5 h: (a) at temperatures indicated with 15 MPa pressure; (b) at 1650°C with pressures indicated.

The microstructure of mullite derived from kaolinite/ α -alumina powder hot pressed at 1600°C for 1.5 h with 15 MPa pressure is shown in Fig. 5. The microstructure consisted of a bimodal grain size, of larger (length/width = $4.1 \pm 0.5/0.9 \pm 0.3 \mu\text{m}$) elongated primary mullite grains, and smaller ($1 \pm 0.4 \mu\text{m}$), more equiaxed secondary mullite grains. EDS of the glassy phase at grain boundaries indicated Si and K originating from the raw materials.

The distribution of the platelets in composites was generally uniform, with only occasional areas showing agglomerates, as seen in Fig. 6. The grain size of mullite in the sol-gel derived composite was the same as that of the single phase hot pressed mullite ($1.7 \pm 0.3 \mu\text{m}$). Interfacial voids were associated with the larger platelets, but largely absent with the smaller ones. Thermal expansion mismatch between reinforcement and matrix generates local internal stress in these composites which causes

microcracking (Fig. 7). TEM of the composite (Fig. 8) shows a thin (10–70 nm) glassy phase at mullite–SiC interfaces.

3.3 Mechanical properties

Figure 9(a) shows the sol-gel mullite composite fracture toughness as a function of SiC platelet loading after hot-pressing 1.5 h at 1650°C with 15 MPa pressure. Fracture toughness increased with increasing volume fraction of SiC platelets. The increase in K_{IC} for mullite derived from sol-gel powder with 20 vol% SiC platelets ($3.9 \pm 0.1 \text{ MPa m}^{1/2}$) was about 35% over that of monolithic mullite derived from sol-gel powder ($2.9 \pm 0.1 \text{ MPa m}^{1/2}$). The addition of SiC enhanced the K_{IC} of the composites. SEM images of the polished surfaces of the mullite and mullite with 20 vol% SiC platelets after Vickers indentations are shown in Fig. 10. Clearly, crack branching and deflection around the SiC platelets are present, but little evidence of

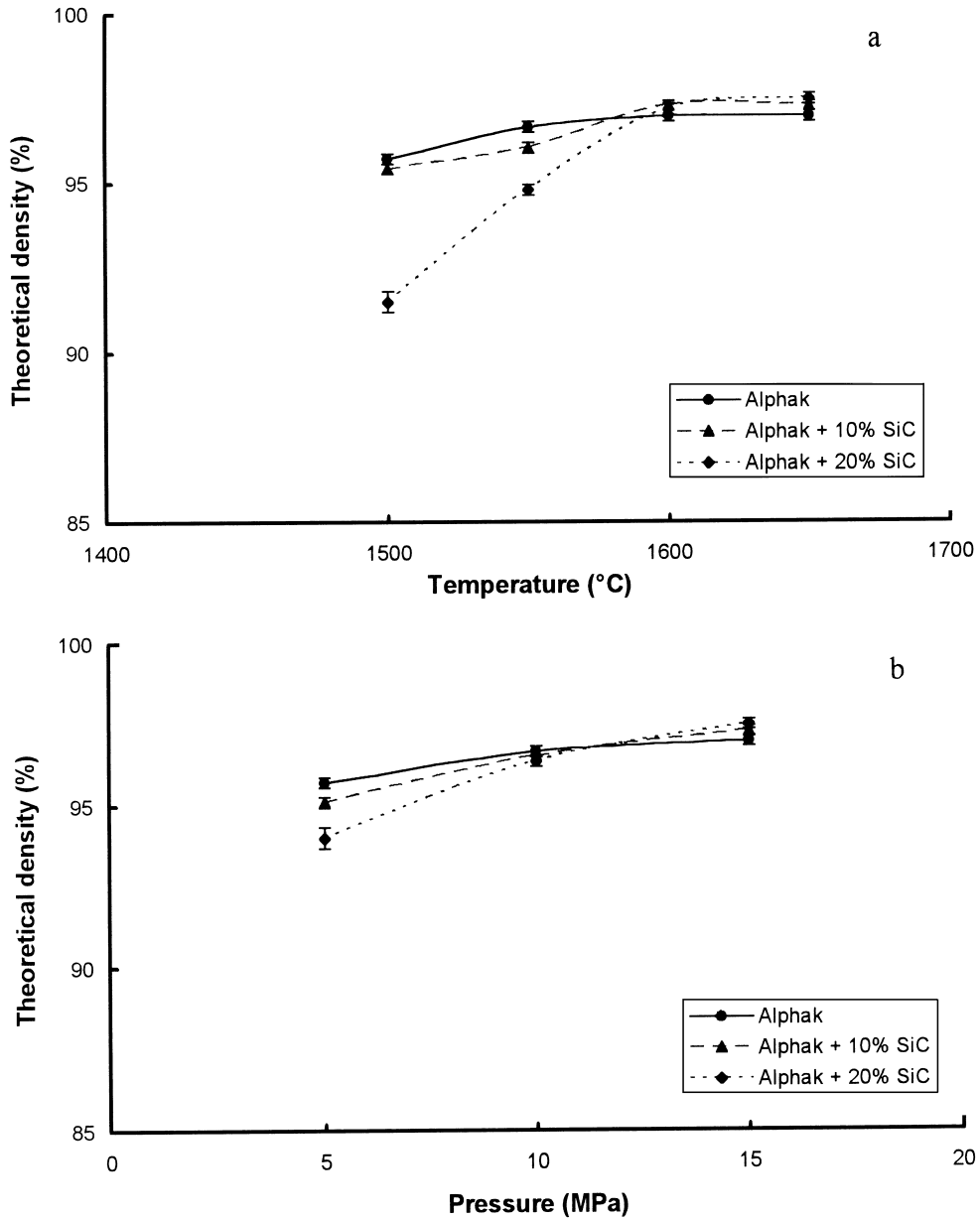


Fig. 3. Bulk density of mullite pellets derived from clay/ α -alumina powder (Alphak) hot pressed 1.5 h: (a) at temperatures indicated with 15 MPa pressure; (b) at 1600°C with pressures indicated.

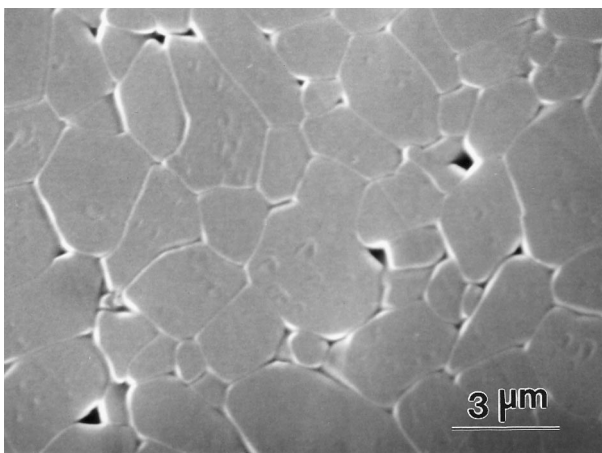


Fig. 4. SEM micrograph of mullite pellets hot-pressed 1.5 h at 1650°C with 15 MPa pressure.

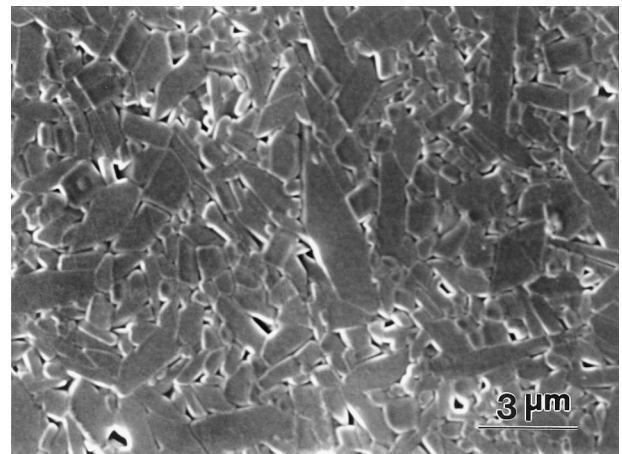


Fig. 5. SEM micrograph of mullite pellets derived from kaolinite/ α -alumina powder hot pressed 1.5 h at 1600°C with 15 MPa pressure.

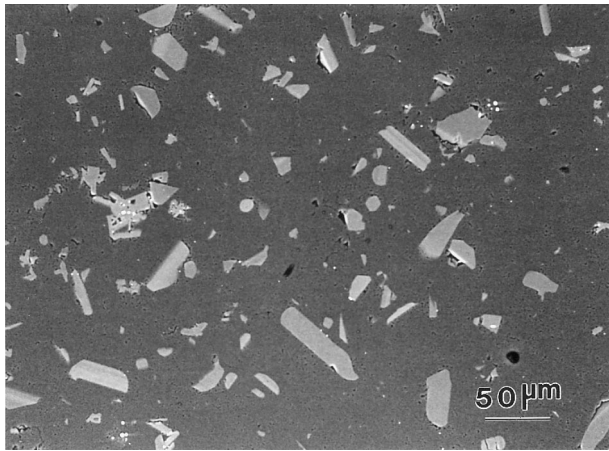


Fig. 6. Backscattered electron SEM image of SiC distribution in composites derived from sol-gel powder after 1.5 h at 1650°C with 15 MPa pressure with 10% SiC platelets (hot-pressing direction is perpendicular to the plane of the paper).



Fig. 7. TEM of microcrack (arrowed) at the interface between SiC platelets and mullite derived from kaolin/ α -alumina hot pressed 1.5 h at 1600°C with 15 MPa pressure.

crack bridging was found. The fracture surfaces showed evidence of crack deflection and, in some places, the platelets break along the fracture path.

The fracture toughness of mullite derived from kaolinite/ α -alumina with SiC platelet reinforcement is shown in Fig. 9(b). The increase in K_{IC} of mullite derived from kaolinite/ α -alumina with 20 vol% SiC platelets ($3.7 \pm 0.1 \text{ MPa m}^{1/2}$) compared with monolithic mullite derived from kaolinite/ α -alumina ($2.9 \pm 0.1 \text{ MPa m}^{1/2}$) was about 30%, but the toughness of mullite derived from kaolinite/ α -alumina with 20 vol% SiC platelets was nearly the same as with sol-gel powder with 20 vol% SiC platelets ($3.9 \pm 0.1 \text{ MPa m}^{1/2}$). SEM observations of the polished surfaces of the mullite with 10 and 20 vol% SiC platelets showed that branching and deflection toughening mechanisms were active.

SEM of the fracture surfaces after bend testing (Fig. 11) are consistent with the observations of the cracks around the indents (Fig. 10). The fracture

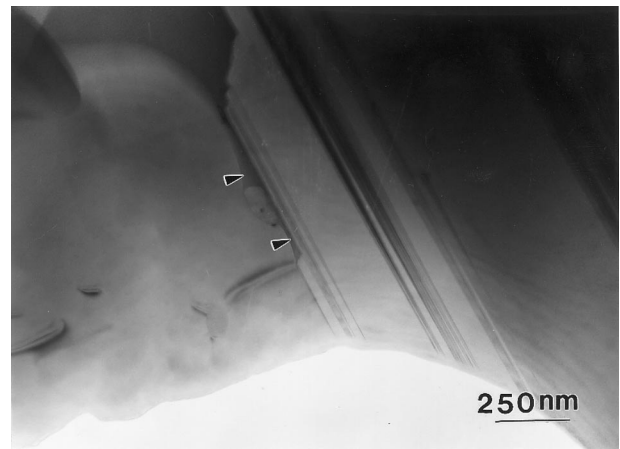


Fig. 8. TEM image of glassy phase (arrowed) at interface between SiC platelets and mullite matrix derived from sol-gel after 1.5 h at 1650°C with 15 MPa pressure.

surface of the composite was macroscopically rougher than the monolith for both process routes. Evidence of crack deflection and branching was found although in many cases crack propagation was directly through the SiC.

Vickers hardness increased with increasing volume fraction of SiC platelets for both sol-gel and kaolinite/ α -alumina mullite (Figs 12 and 13). The hardness of mullite derived from kaolinite/ α -alumina was slightly less than mullite derived from sol-gel powder.

4 Discussion

The highest density for mullite derived from kaolinite/ α -alumina was achieved at lower temperature (1600°C) than mullite derived from sol-gel processing (1650°C). This was due to the presence of the higher levels of (K_2O , Fe_2O_3) impurities in this mullite originating from the raw materials. These impurities flux and lower the viscosity of the liquid phase and significantly increase densification by viscous flow.⁹

Initial densification during the heating cycle to the hot pressing temperature may be rapid because of viscous flow of the liquid phase before mullitisation has occurred. However, after complete mullitisation the densification rate is slow due to the poor solid state sinterability of mullite powder.¹⁰ During hot pressing the applied pressure partly overcomes the resistance to densification and the presence of any silicate liquid at high temperatures after partial mullitisation further facilitates densification. Liquid silicate in the boehmite-derived mullite arises from the 0.02 wt% SiO_2 and 0.007 wt% K_2O in boehmite¹¹ and higher alkali impurities in the kaolin/ α -alumina-derived mullite (Table 1).

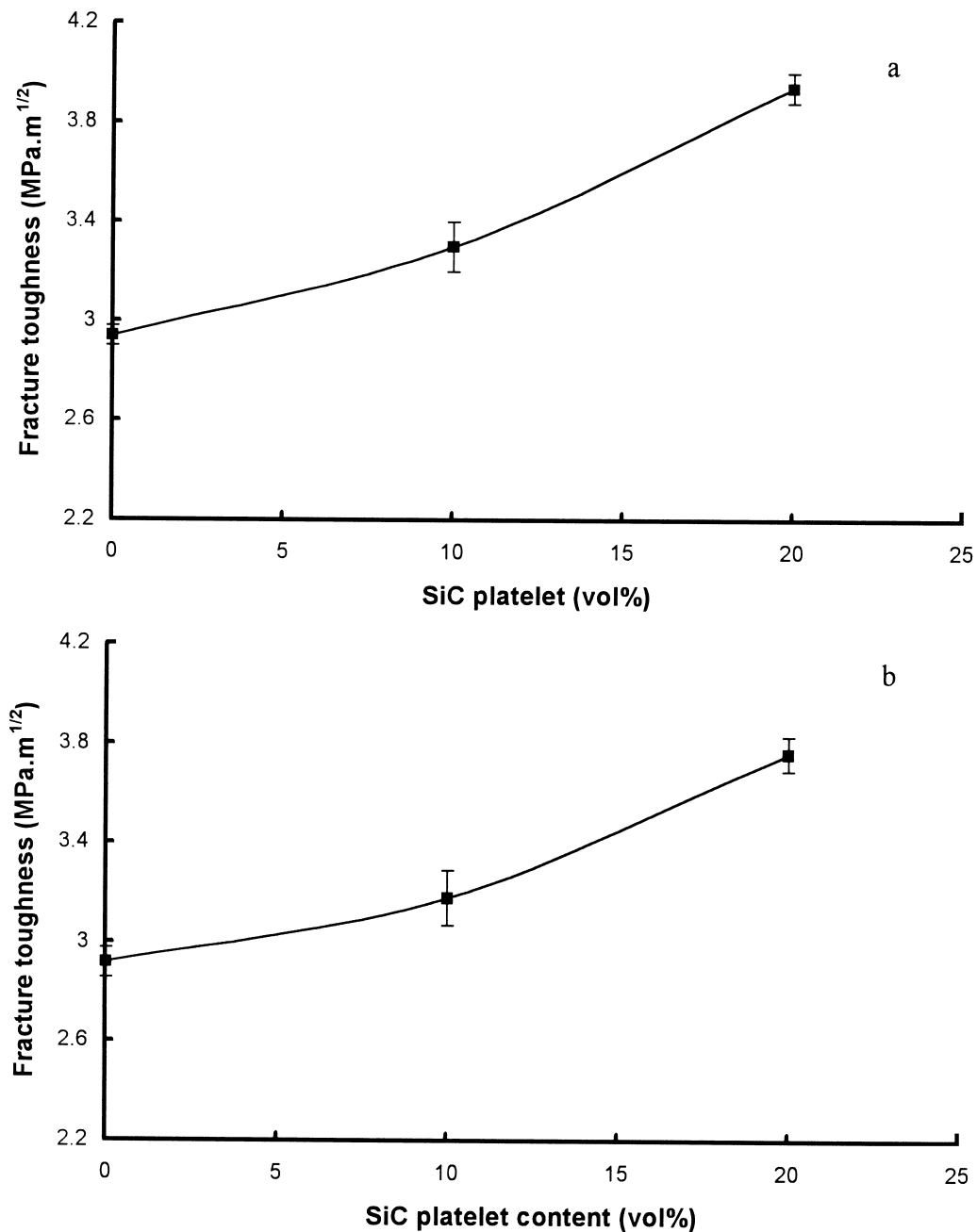


Fig. 9. Fracture toughness of mullite/SiC composites as a function of SiC content: (a) mullite derived from sol-gel powder hot-pressed at 1650°C for 1.5 h with 15 MPa pressure; (b) mullite derived from kaolinite/ α -alumina hot-pressed at 1600°C for 1.5 h with 15 MPa pressure.

The densities achieved here can be compared to Ghate *et al.*¹² who achieved 98.3% of theoretical density when hot pressing γ -alumina (~ 30 nm particles) and silica (~ 13 nm particles) at 1580°C, while Mizuno and Saito¹¹ hot pressed calcined $\text{Al}_2(\text{SO}_4)_3 \cdot 18\text{H}_2\text{O}$ and fumed silica for 1 h at 1600°C and achieved a theoretical density of 97.8%. Seabra *et al.*⁹ hot pressed mullite with 15 MPa pressure at 1600°C for 1 h to give a theoretical density of 97.8%, a similar result to the present study.

Mullite powder compacts have poor sinterability,¹⁰ and sintering of high-purity mullite is rather difficult in the absence of a glassy phase.¹³ Adding SiC further inhibits densification, and this is particularly pronounced with a mullite matrix

which is difficult to densify. Reinforcements such as platelets and whiskers impede composite densification because they inhibit packing and shrinkage.^{14,15} For example, Kamiaka *et al.*¹⁶ found that both the density and toughness fell off rapidly with >10 vol% SiC after pressureless sintering cold isostatically pressed mullite-ZrO₂ composites. Nevertheless, the densification of the composites in the present work is comparable to those obtained by other workers. For example, Sakai *et al.*¹⁷ obtained a maximum density about 98% of theoretical with 30 vol% SiC platelets after hot pressing at 1700°C with 29 MPa pressure.

The processing routes adopted appeared to have given a good distribution of the platelets with

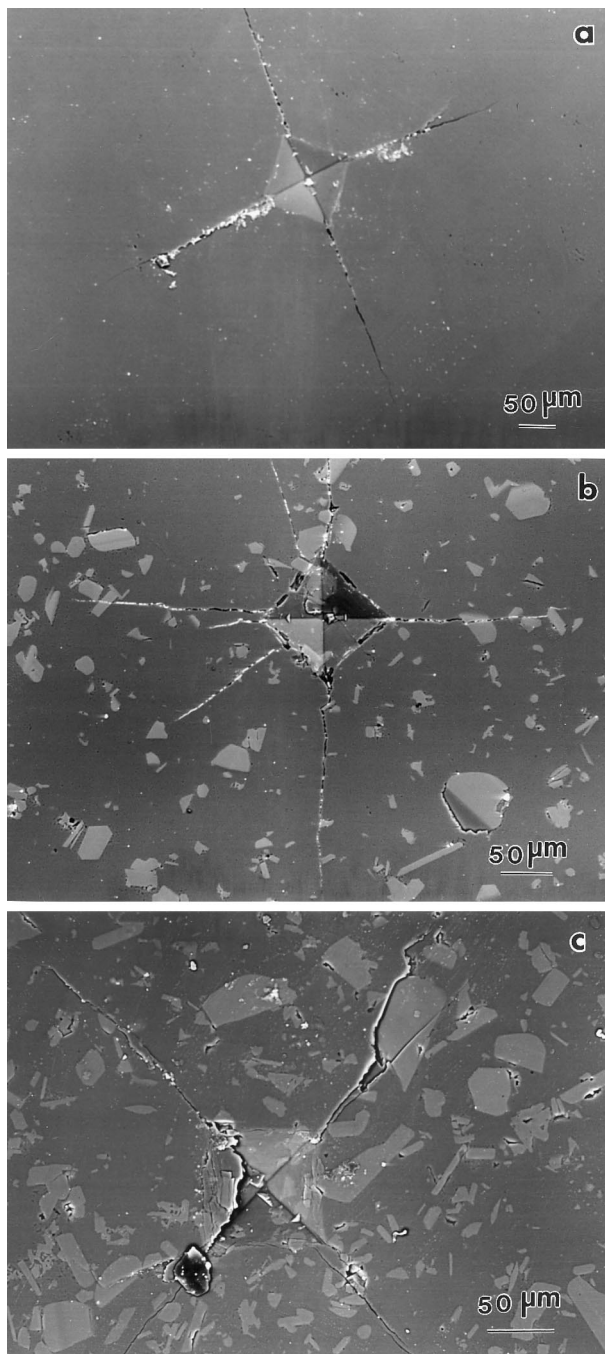


Fig. 10. Vickers indentations made on the surface of hot-pressed samples derived from sol-gel powder: (a) mullite; (b) mullite with 10% SiC platelets; (c) mullite with 20% SiC platelets.

minimal agglomeration. For both routes TEM (e.g. Fig. 8) showed a thin layer of glassy phase at the SiC–mullite interface. The small amount of silica impurity from the platelets plays an important role in the formation of liquid phases at high temperatures which act as sintering aids for the composites.¹⁸ Where agglomeration did occur, porosity was present of a size (2–5 μm) which scaled with the agglomerate size (interfacial voids also were seen associated with the larger platelets).

The room temperature K_{IC} for mullite derived from sol-gel processing with 20 vol% SiC platelets

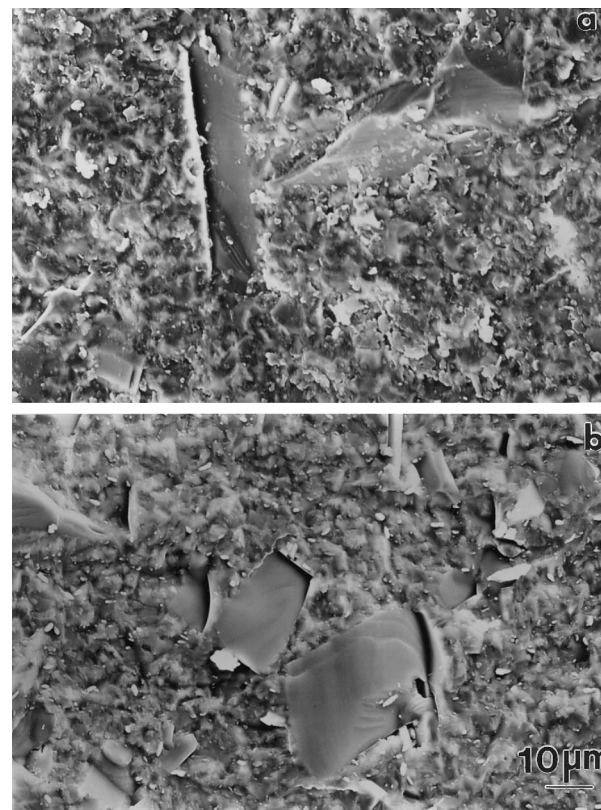


Fig. 11. Fracture surfaces of mullite with 10 vol% SiC platelets: (a) derived from sol-gel processing after 1.5 h at 1650°C with 15 MPa pressure; (b) derived from kaolin/α-alumina after 1.5 h at 1600°C with 15 Pa pressure.

was $3.9 \pm 0.1 \text{ MPa m}^{1/2}$ which was larger than the value reported by Seabra *et al.*⁹ ($2.4 \pm 0.2 \text{ MPa m}^{1/2}$) who used commercial mullite with 22.5 vol% SiC platelets, and also Sakai *et al.*¹⁷ ($3.4 \text{ MPa m}^{1/2}$) who used mullite with 30 vol% SiC platelets. Nischik *et al.*¹⁸ obtained a fracture toughness of about $3.3 \pm 0.3 \text{ MPa m}^{1/2}$ for a 10% SiC addition, which is comparable to the figure for the present study ($3.3 \pm 0.1 \text{ MPa m}^{1/2}$) for mullite–10% SiC derived from sol-gel powder.

The fracture toughness of the kaolinite/α-alumina was consistently lower than the values obtained from the sol-gel derived material. Nevertheless, the values in the present study may be regarded as high for material derived from kaolinite. For example, Takada *et al.*¹⁹ using natural mullite derived from kaolinite–alumina obtained a toughness of $2 \text{ MPa m}^{1/2}$ for the monolith and 2.5 to $3 \text{ MPa m}^{1/2}$ for 10 and 15 vol% SiC powder composites, respectively. It is probable that the difference in the fracture toughness arises from the different processing routes since Takada *et al.*¹⁹ used pressureless sintering at 1700°C.

Irrespective of the processing route, a significant increase in toughness with SiC addition was found (Fig. 9). This was also associated with an increased tortuosity of the crack path with increased SiC addition (Figs 10 and 11). The toughening effect in

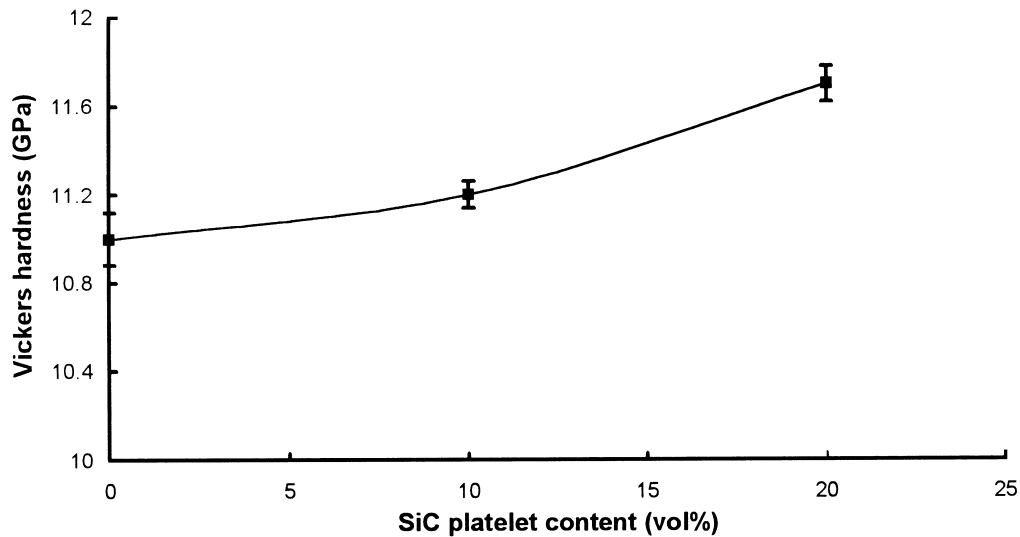


Fig. 12. Vickers hardness of sol-gel derived mullite/SiC composites as a function of SiC content (hot-pressed 1.5 h at 1600°C and 15 MPa).

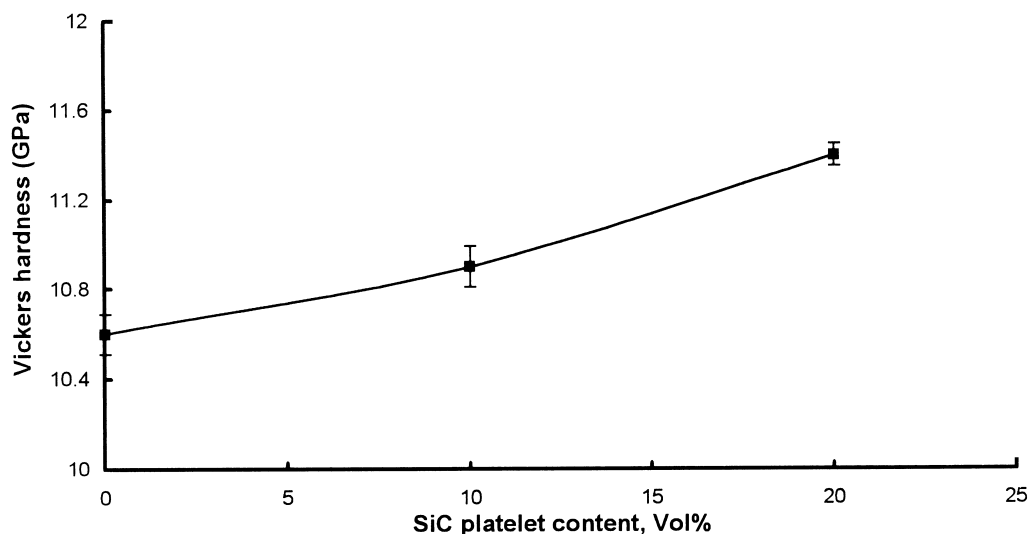


Fig. 13. Vickers hardness of clay/ α -alumina derived mullite/SiC composites as a function of SiC content (hot-pressed 1.5 h at 1600°C and 15 MPa).

composites is strongly controlled by the reinforcement/matrix interface.^{20–22} Increases in fracture toughness have been attributed to two principal mechanisms in platelet-reinforced composites.²³ Firstly, crack deflection by the platelets.¹⁸ This mechanism was apparent, particularly associated with the larger SiC platelets, for example Fig. 10(c). Secondly, modulus-load-transfer¹⁸ is believed to increase toughness by transferring stresses at a crack tip to regions remote from the crack tip, so decreasing the stress intensity at the crack tip. There is clearly potential for this toughening mechanism in the SiC/mullite system since the elastic modulus of the reinforcing component (~ 450 GPa) is more than twice that of the matrix (~ 200 GPa).²⁴ However, the weak interface between reinforcement and platelet, as demonstrated by the

significant amount of crack deflection, will have reduced the extent of toughening by modulus transfer. With the experimental results presented here, there is no quantitative method for separating the relative contributions of these two mechanisms. Nevertheless, microstructural observations strongly suggest that crack deflection was the dominant toughening mechanism.

The increase in fracture toughness with SiC addition was less in mullite derived from kaolinite/ α -alumina with addition of SiC platelets (total increment $0.8 \text{ MPa m}^{1/2}$) than mullite derived from sol-gel processing (total increment $1.0 \text{ MPa m}^{1/2}$). There were two principal differences between the microstructures; the greater glassy phase content, and grain shape heterogeneity of the kaolinite material. The first effect may be expected to reduce

toughness through the inherently low K_{IC} of glass ($\sim 1 \text{ MPa m}^{1/2}$), while the second would be expected to increase toughness by promoting crack deflection, provided fracture was intergranular. Since toughness was lower in the kaolinite derived material, it would appear that the increased glass content was the dominant microstructural difference determining toughness.

SEM and TEM observations revealed microcracks at the interface of mullite and SiC platelets, believed to be a result of the thermal expansion mismatch between reinforcement and matrix when cooling from the processing temperature to room temperature. The thermal expansion of mullite is $5.5 \times 10^{-6}/^\circ\text{C}$ and SiC $4.5 \times 10^{-6}/^\circ\text{C}$ ($0\text{--}1000^\circ\text{C}$),²⁵ respectively. On cooling to room temperature from the processing temperature (1650°C), a tensile stress should be induced in the matrix and compressive stress in the reinforcement, resulting in the generation of microcracking at the matrix-reinforcement interface. Microcracking will have promoted crack deflection which may have been expected to increase the toughness of the composites, an effect previously reported.^{18,26,27} However, for mullite derived from kaolinite/ α -alumina with greater glassy phase, residual stresses could be accommodated in the viscous glass, reducing the extent of microcracking.

Vickers hardness increased with increasing volume fraction of SiC platelets for both mullite derived from sol-gel processing and kaolinite/ α -alumina (Figs 12 and 13). This is a result of the higher hardness of SiC (22 GPa) compared to mullite (14 GPa).¹ The maximum density achieved, 97.5% of theoretical density, resulted in a significant fraction of pores ($2\text{--}5 \mu\text{m}$) which reduce hardness.¹ The hardness of mullite pellets derived from sol-gel powder was higher than mullite pellets derived from kaolinite/ α -alumina, probably a result of the greater glassy content of the latter.

5 Conclusions

Density of mullite, and mullite with 10 and 20 vol% silicon carbide platelets, from hot-pressed sol-gel powder increased with increasing hot pressing temperature ($1550\text{--}1650^\circ\text{C}$). Maximum density (97.5% of theoretical density) was achieved after 1.5 h at 1650°C with 15 MPa pressure. The presence of SiC platelets hinders densification.

Density of mullite and mullite with 10 and 20 vol% SiC platelet addition from hot pressed kaolinite/ α -alumina powder increased with increasing temperature ($1500\text{--}1600^\circ\text{C}$), but levelled off above this temperature. Again, a decrease in density was found as platelet addition increased.

A maximum density of 97.5% of theoretical was achieved after 1.5 h at 15 MPa pressure at 1600°C .

Maximum density for mullite and mullite with 10 and 20 vol% SiC platelets derived from kaolinite/ α -alumina occurred at a lower temperature (1600°C) than mullite and mullite with 10 and 20 vol% SiC platelets derived from sol-gel processing (1650°C).

In the sol-gel mullite composites, fracture toughness increased with increasing volume fraction of SiC platelets after hot-pressing 1.5 h at 1650°C with 15 MPa pressure. The increase in K_{IC} for mullite derived from sol-gel powder with 20 vol% SiC platelets was about 35% over monolithic mullite derived from sol-gel powder.

Fracture toughness of mullite derived from kaolinite/ α -alumina with 20 vol% SiC platelets after hot-pressing 1.5 h at 1600°C with 15 MPa pressure increased with increasing volume fraction of SiC platelets. The increase in K_{IC} of mullite with 20 vol% SiC platelets over monolithic mullite derived from kaolinite/ α -alumina was about 30%.

SEM observation of fracture surfaces after bend tests showed that crack deflection around the platelets probably made a significant contribution to the fracture toughness of the composites, although in several places the crack propagated through the platelets. There was little evidence of crack bridging.

References

1. Lee, W. E. and Rainforth, W. M., In *Ceramic Microstructures, Property Control by Processing*, Chapman and Hall, London, 1994, pp. 290–311.
2. Tieg, T., Becher, P. and Angelini, P., Microstructure and properties of SiC whisker-reinforced mullite composites. In *Ceramic Transactions, Vol. 6, Mullite and Mullite Matrix Composites*, ed. S. Somiya, R. F. Davis and J. A. Pask. American Ceramic Society, Westerville, OH, 1990, pp. 463–472.
3. Birchall, J. D., Stanley, D. R., Mockford, M. G., Pigott, G. H. and Pinto, P. J., Toxicity of silicon carbide whiskers. *J. Mater. Sci. Lett.*, 1988, **7**, 350–352.
4. Rezaie, H. R., Rainforth, W. M. and Lee, W. E., Mullite evolution in ceramics derived from kaolinite, kaolinite with added α -alumina, and sol-gel precursors. *Brit. Ceram. Trans.*, 1997, **96**(5), 181–187.
5. Vander Voort, G. F., *Metallography*. McGraw-Hill, New York, 1984, pp. 445–446.
6. Anstis, G. R., Chantikul, P., Lawn, B. R. and Marshall, D. B., A critical evaluation of indentation techniques for measuring fracture toughness: I, direct crack measurements. *J. Am. Ceram. Soc.*, 1981, **64**(9), 533–538.
7. Chantikul, P., Anstis, G. R., Lawn, B. R. and Marshall, D. B., A critical evaluation of indentation techniques for measuring fracture toughness: II, strength method. *J. Am. Ceram. Soc.*, 1981, **64**(9), 539–543.
8. Lawn, B. R., In *Fracture of Brittle Solids*, 2nd edn. Cambridge University Press, Cambridge, UK, 1993, pp. 249–306.

9. Mizuno, M., Shiraishi, M. and Saito, H., Microstructure and bending strength of highly pure mullite ceramics. *Ceramic Transactions, Vol. 6, Mullite and Mullite Matrix Composites*, ed. by S. Somiya, R. F. Davis and J. A. Pask. American Ceramic Society, Westerville, OH, 1990, pp. 413–424.
10. Pask, J. A., Zhang, X. W., Tomsia, A. P. and Yoldas, B. E., Effect of sol-gel mixing on mullite microstructure and phase equilibria in the α -Al₂O₃-SiO₂ system. *J. Am. Ceram. Soc.*, 1987, **70**(10), 704–707.
11. Mizuno, M. and Saito, H., Preparation of highly pure fine mullite powder. *J. Am. Ceram. Soc.*, 1989, **72**(3), 377–382.
12. Ghate, B. B., Hasselman, D. P. H. and Spriggs, R. M., Synthesis and characterisation of high purity, fine grained mullite. *Am. Ceram. Soc. Bull.*, 1973, **52**(9), 670–672.
13. Kanzaki, S. and Tabata, H., Sintering and mechanical properties of stoichiometric mullite. *J. Am. Ceram. Soc.*, 1985, **68**, C–6–C-7.
14. Zhang, Z., Huang, Y., Zheng, L. and Jiang, Z., Preparation and mechanical properties of SiC whisker and nano-sized mullite particulate reinforced TZP composites. *J. Am. Ceram. Soc.*, 1996, **79**(10), 2770–2782.
15. Samanta, S. C. and Musikant, S., SiC whiskers-reinforced ceramic matrix composites. *Ceram. Eng. Sci. Proc.*, 1985, **6**(7–8), 663–672.
16. Kamiaka, H., Yamagishi, C. and Asaumi, J., Mechanical properties and microstructure of mullite-SiC-ZrO₂ particulate composite. *Ceramic Transactions, Vol. 6, Mullite and Mullite Matrix Composites*, ed. S. Somiya, R. F. Davis and J. A. Pask. American Ceramic Society, Westerville, OH, 1990, pp. 509–518.
17. Sakai, H., Matsuhiro, K. and Furuse, Y., Mechanical properties of SiC platelet reinforced ceramic composites. *Ceramic Trans.*, 1991, **19**, 765–771.
18. Nischik, C., Seibold, M. M., Travitzky, N. A. and Clausen, N., Effect of processing on mechanical properties of platelet-reinforced mullite composites. *J. Am. Ceram. Soc.*, 1991, **74**(10), 2464–2468.
19. Takada, H., Nakahira, A., Ohnishi, H., Kawanami, T. and Niihara, K., Fabrication and evaluation of natural mullite composites. *J. Japan. Soc. of Powder and Powder Metallurgy*, 1990, **37**(7), 1060–1062.
20. Sheppard, L. M., Trends in HIP equipment capabilities. *Am. Ceram. Soc. Bull.*, 1992, **71**(3), 323–327.
21. Kerans, R. J., Hay, R. S. and Pagano, N. J., The role of the fibre-matrix interface in ceramic composites. *Am. Ceram. Soc. Bull.*, 1989, **8**(2), 429–442.
22. Singh, R. N. and Gaddipati, A. R., Mechanical properties of a uniaxially reinforced mullite-silicon carbide composite. *J. Am. Ceram. Soc.*, 1988, **71**(2), C–100–C103.
23. Warren, R., *Ceramic-Matrix Composites*. Blackie and Son, Glasgow. Chapman and Hall, New York, 1992.
24. Heussner, K. H. and Claussen, N., Yttria-and ceria-stabilised tetragonal zirconia polycrystals (Y-TZP, Ce-TZP) reinforced with Al₂O₃ platelets. *Journal of the European Ceramic Society*, 1989, **5**, 193–200.
25. Wadsworth, I. and Stevens, R., Strengthening and toughening of cordierite by the addition of silicon carbide whiskers, platelets and particles. *J. Mater. Sci.*, 1991, **26**, 6800–6808.
26. Boecker, W. D. G., Chwastiak, S., Frechette, F. and Lau, S., Single phase alpha-SiC reinforcements for composites. In *Ceramic Trans., Vol. 2., Silicon Carbide*, 87, ed. by J. D. Cawley and C. E. Semler. American Ceramic Society, Westerville, OH, 1989, pp. 407–420.
27. Rice R. W., Microstructure dependence of mechanical behaviour of ceramics. In *Treatise on Materials Science and Technology, Vol. 11, Properties and Microstructure*, Academic Press, New York, 1977, pp. 199–381.